Autor/s

Dra. Pilar Marco Buj
Departament Enginyeria Química i Química Analítica

Grau en Enginyeria Química

Treball Final de Grau

Feasibility Study of Hydrochar/Zn composites in Heterogeneous Photocatalytic Degradation

Lina Hu

June 2024

UNIVERSITAT DE BARCELONA

En primer lugar, queiro agradecer a mis tutores Pilar Marco y Julio César, por su dedicación y el invaluable apoyo que me han brindado durante estos meses, lo que me ha permitido terminar con mi Trabajo de Fin de Grado.

También quiero agradecer a mis familiares, especialmente a mi madre, mi hermana, mi prima, mis mejores amigas y mis mejores compañeros de la universidad, quienes me han acompañado y apoyado a lo largo de toda mi etapa universitaria.

Finalmente, un agradecimiento especial a mis mascotas, LiuLiu y Wilson, cuyo cariño y compañía han sido una fuente constante de alegría y motivación para mí.

CONTENTS

SUMMARY I

RESUM III

SUSTAINABLE DEVELOPMENT GOALS V

1. INTRODUCTION 1
1.1. GENERAL CONTEXT IN CATALONIA 1
1.1.1. Wine sector 1
1.1.2. Drought problem 2
1.2. EMERGING POLLUTANTS IN WASTEWATER 3
1.2.1. Thiacloprid 5
1.2.2. Metoprolol 6
1.3. ADVANCED OXIDATION PROCESSES (AOPs) 7
1.3.1. Heterogeneous photocatalytic degradation 9
1.3.1.1. Hydrozincite ($HDZn/Zn_5(CO_3)_2(OH)_6$) 12
1.4. HYDROCHAR 13
1.4.1. Hydrothermal Carbonization (HTC) 14
1.4.2. Application of hydrochar in adsorption 15
1.4.3. Application of hydrochar in photocatalysis 16

2. OBJECTIVES 19

3. EXPERIMENTAL 21
3.1. SYNTHESIS OF MATERIALS 21
3.1.1. Synthesis of HDZn 21
3.1.2. Synthesis of HC 22
3.1.3. Synthesis of HC-HDZn 23
3.1.4. Synthesis of HC-ZnN_2O_6 23
3.2. EXPERIMENTAL DESIGN 24
3.3. EXPERIMENTAL PROCEDURE 26
3.3.1. Process of photodegradation 26
3.3.2. Reusability cycles in photocatalytic degradation 27

4. RESULTS AND DISCUSSION 29
4.1. CALIBRATION 29

4.2. EVALUATION OF THE EFFECTIVENESS OF COMPOSITES IN THE ADSORPTION PROCESS 31
4.3. EFFECTIVENESS OF INDIVIDUAL HC ON PHOTODEGRADATION 33
4.4. ANALYSIS OF METOPROLOL PERCENTAGE DEGRADATION 36
4.5. ANALYSIS OF THIACLOPRID PERCENTAGE DEGRADATION 38
4.6. POLLUTANT DEGRADATION COMPARISON USING THE OPTIMAL PHOTOCATALYST 40
4.7. ANALYSIS OF PHOTOCATALYST REUSABILITY IN MULTIPLEPHOTOCATALYTIC DEGRADATION CYCLES 41
5. CONCLUSIONS 43
REFERENCES AND NOTES 45
ACRONYMS 49
APPENDICES 51
APPENDIX 1: TABLE OF CONTAMINANT CONCENTRATIONS 53
APPENDIX 2: ANALYSIS OF THE BAND GAP ENERGY OF HC-HDZN 55

SUMMARY

Water pollution has become an increasingly severe environmental problem. This increase is due to industrial factors and the growing demand for water by the population. This situation is aggravated by the drought problem in Catalonia, which intensifies the pressure on available water resources.

With its rich wine-growing tradition, Catalonia generates a large amount of agricultural waste after the grape harvest each year, mainly from the vine shoots. These residues can be converted into hydrochar (HC), a material that is effective in adsorption and photocatalysis processes when combined with other oxides.

Considering these factors, interest arises in recycling organic waste into hydrochar (HC) and using it in heterogeneous photocatalytic degradation processes (one of the AOPs techniques) to eliminate emerging pollutants. This approach offers a more sustainable, economical and ecological solution to address drought and improve water quality.

This project is proposed to evaluate the feasibility and efficiency of HC and HC/Zn composites in the photodegradation of metoprolol and thiacloprid pollutants under UV irradiation. The aim was to synthesize these composites and analyze their photocatalytic effectiveness and their reusability through multiple degradation cycles.

The results showed that individual HC achieved a significant degradation percentage, with 19.91% for metoprolol and 16.89% for thiacloprid after 3 hours of UV illumination.

Among the synthesized photocatalysts, HC-HDZn 10% achieved the highest photocatalytic activity, reaching degradation efficiencies of 99.82% for metoprolol and 98.27% for thiacloprid.

The study also analyzed the reuse of the optimal photocatalyst in multiple degradation cycles, showing a slight decrease in efficiency but maintaining more than 90% of its initial capacity after three cycles.

These results indicate that HC and its composites are promising materials in the photodegradation of organic pollutants, proving successful in environmental remediation applications due to their sustainable, stable character and high efficiency.

Future studies could further optimize these materials and explore their application to a wider variety of pollutants.

Keywords: Hydrochar, Hydrozincite, HC-HDZn, Photodegradation, Wastewater, Advanced Oxidation Processes, Emerging contaminants, Metoprolol, Thiacloprid.

RESUMEN

La contaminación del agua se ha convertido en un problema medioambiental cada vez más grave. Este aumento se debe tanto a factores industriales como a la creciente demanda de agua por parte de la población. Esta situación se ve agravada por la problemática de la sequía en Cataluña, que intensifica la presión sobre los recursos hídricos disponibles.

Cataluña, con su rica tradición vitivinícola, genera una gran cantidad de residuos agrícolas tras la cosecha de uvas cada año, principalmente de los sarmientos de la vid. Estos residuos pueden ser convertidos en hydrochar (HC), un material que ha mostrado ser eficaz en procesos de adsorción y fotocatálisis cuando se combina con otros óxidos.

Considerando estos factores, surge el interés por el reciclaje de residuos orgánicos para convertirlos en hydrochar (HC) y aprovecharlos en procesos de degradación fotocatalítica heterogénea (una de las técnicas de los AOPs) con el fin de eliminar contaminantes emergentes. Este enfoque busca ofrecer una solución más sostenible, económica y ecológica para abordar la situación provocada por la sequía y mejorar la obtención de agua de calidad.

Se propone este proyecto con el objetivo de evaluar la viabilidad y eficiencia de HC y compuestos de HC/Zn en la fotodegradación de los contaminantes metoprolol y thiacloprid bajo irradiación UV. Se plantea sintetizar estos compuestos, analizar su efectividad fotocatalítica y su capacidad de reutilización a través de múltiples ciclos de degradación.

Los resultados obtenidos mostraron que el HC individual logró porcentaje de degradación significativas, con un 19.91% para el metoprolol y un 16.89% para el thiacloprid después de 3 horas de iluminación UV.

Entre los fotocatalizadores sintetizados, el HC-HDZn 10% logró la mayor actividad fotocatalítica, alcanzando eficiencias de degradación del 99.82% para el metoprolol y del 98.27% para el thiacloprid.

El estudio también analizó la reutilización del fotocatalizador óptimo en múltiples ciclos de degradación, demostrando una ligera disminución en la eficiencia, pero manteniendo más del 90% de su capacidad inicial tras tres ciclos.

Estos resultados indican que el HC y sus compuestos son materiales prometedores en la fotodegradación de contaminantes orgánicos, demostrando ser exitosos en la aplicación para la remediacion ambiental debido a su carácter sostenible, estable y alta eficiencia.

Futuros estudios podrían optimizar aún más estos materiales y explorar su aplicación en una variedad más extensa de contaminantes.

Palabras claves: Hydrochar, Hydrozincite, HC-HDZn, Fotodegradación, Aguas residuales, Procesos de Oxidación Avanzada, Contaminantes emergentes, Metoprolol, Thiacloprid.

SUSTAINABLE DEVELOPMENT GOALS

This study on the feasibility of hydrochar/Zn composites in heterogeneous photocatalytic degradation can impact areas of People and Planet and contributes directly to several Sustainable Development Goals (SDGs):

- SDG 6: Clean Water and Sanitation. Efficient wastewater treatment ensures the use of clean water after treatment.
- SDG 12: Responsible Consumption and Production. Using waste to produce sustainable and environmentally friendly materials is behavior that contributes to responsible consumption and production.
- SDG 13: Climate Action. The treatment of wastewater and its transformation into drinkable water resources is an action to combat the problem of drought.
- SDG 15: Life on Land. By reducing pollution from persistent toxic pollutants in the environment, this research helps to protect aquatic and terrestrial ecosystems.

1. INTRODUCTION

1.1. GENERAL CONTEXT IN CATALONIA

1.1.1. Wine sector

For more than 2,300 years, wine has been an integral part of Catalan culture, making the viticulture industry a major participant in the region's food and agriculture sectors.

With over 800 wineries, 650 of which fall under a Denomination of Origin (DO), this industry employs over 25,000 people, underscoring its significance for Catalonia's economy and society. [1, 2]

In 2022, wine from Catalonia's Designations of Origin (DO) brought in 346.6 million euros in sales worldwide. This number is supported by the annual production of 88.7 million fine wine bottles.[3]

The Catalan region boasts almost 56,000 hectares of vineyards, ranking fifth among the autonomous communities in terms of vineyard extension, which is a testament to the strong market demand for wine. [4]

Pruning the vine after grape harvest is a standard practice to control overgrowth and get it ready for the following growing season. However, this method produces a significant amount of agricultural organic waste because of the volume of wine produced annually.

There are various methods for managing waste; controlled burning is one of them, however it may not be the best for the environment. Utilizing the residue as composting material is an additional option that enables them to be transformed into beneficial organic fertilizer that can enhance soil quality and lessen the need for chemical fertilizers.

Furthermore, leftover vine pruning material can be recycled into handicraft items or utilized as biomass to clean water.

When mixed and chemically treated with certain metal oxides, biomass made from organic waste (in this example, grape vine shoots) may be able to break down organic contaminants found in wastewater, aiding in the natural and cost-effective cleaning of water. It provides the chance to repurpose these wastes as fresh resources in a more environmentally friendly manner.

1.1.2. Drought problem

A region faces severe water scarcity for an extended length of time during a drought, which is typically brought on by below-average rainfall. This issue causes a mismatch between the amount of water that is naturally available and the amount that is required due to human activities.

Because of the Mediterranean environment, rainfall in Catalonia is erratic, with extended periods of scarcity interspersed with bursts of heavy rain.

Due to this unpredictability, there is a drought problem, particularly in the interior basins where over 80% of the population lives and only 40% of Catalonia's total water supply—primarily from reservoirs and aquifers—is accessible. Rivers, streams, and rainfall provide the water for reservoirs, which is further augmented by aquifer water, repurposed sewage system water, and regeneration station water.[5]

The present severe drought, which has been going on for more than 36 months without rain and is affecting the years 2021–2023, is the worst that Catalonia has experienced since records have been kept in 1905. [6]

In Catalonia, there are nine reservoirs, among which the Susqueda reservoir (Osor) stands out for its remarkable capacity, reaching 233 hm^3. In May 2020, this reservoir had a volume of 222.39 hm^3, which represented 95.4% of its total capacity. However, by May 2024, this percentage has been drastically reduced to 26.7%.

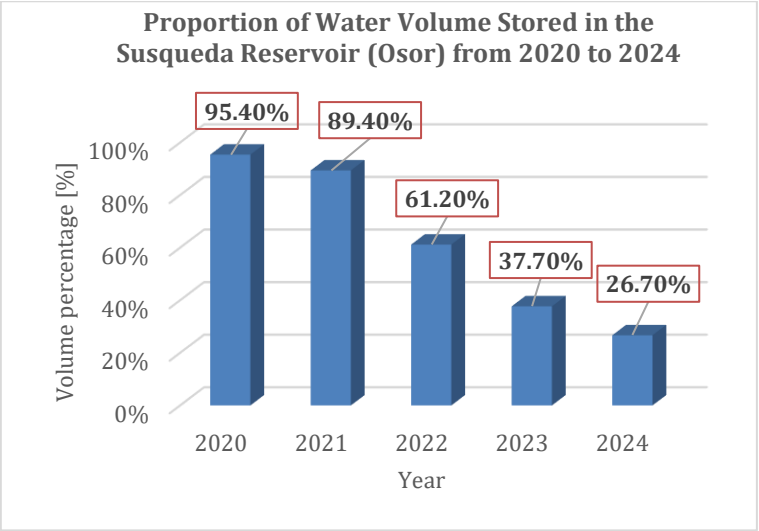

Fig 1. Variations in the Susqueda Reservoir's (Osor) Water Volume in May of Each Year [7]

The reservoirs in the internal basins of Catalonia have a total capacity of 700 hm^3, of which 29.31% is now available. [7]

The scarcity of water resources significantly impacts water supply for domestic use as well as for agricultural and industrial activities. Therefore, wastewater treatment for reuse emerges as a crucial measure. It provides an additional source of water for non-potable applications such as agricultural and industrial irrigation, which contributes to decreasing dependence on limited water sources such as rivers, lakes and aquifers. In addition, this practice frees up available freshwater for priority and critical uses.

Wastewater treatment also plays a crucial role in mitigating environmental impacts. During periods of drought, reduced water flows can place stress on aquatic ecosystems. By reducing the discharge of pollutants in wastewater discharges to receiving water bodies, the process helps to protect both aquatic life and riparian ecosystems.

1.2. EMERGING POLLUTANTS IN WASTEWATER

Water intended for reuse in agricultural and industrial irrigation must be of high quality, as it affects the quality of crops and industrial products.

These quality waters must meet certain quality standards after having undergone appropriate treatments, such as biological treatments that have been widely used in wastewater treatment. However, there are pollutants that are non-biodegradable, recalcitrant and/or toxic, making this type of treatment unusable.

In recent years the presence of emerging pollutants (micropollutants) has become more and more common in various water sources due to the increasing production and use of chemicals such as pharmaceuticals, personal care products (PPCPs), pesticides and industrial chemicals, among others.

As novel contaminants that have not previously been considered hazardous, they are not regulated in drinking water. However, even at very low concentrations (in the order of ng/L), they can cause adverse effects on human health, aquatic ecosystems and biodiversity.

Among the emerging pollutants, persistent organic pollutants (POPs) can be identified, which are released into various aquatic systems from industrial sources or chemical discharges.

Persistent organic pollutants (POPs) are non-biodegradable composites with a high resistance to biological degradation. These pollutants can persist in the environment for long periods, accumulating in the tissues of living organisms and biomagnifying along the food chain, causing adverse effects on human health and ecosystems.

POPs encompass a variety of substances such as pesticides, solvents and detergents, including specific molecules such as metoprolol and thiacloprid.

These contaminants are often difficult to remove by conventional water treatment methods such as sedimentation, filtration, chlorination or disinfection. Therefore, it is necessary to develop and implement advanced technologies, such as advanced oxidation, reverse osmosis, activated carbon adsorption, among other innovative methods.

However, among the advanced technologies, activated carbon adsorption is not recommended for wastewater treatment. Firstly, the cost of activated carbon is high, between 2.2 and 3 $/kg, and regeneration of activated carbon can cost up to 80% of its original price, making it economically unviable. More importantly, once the activated carbon has adsorbed the pollutants, they remain on its surface, meaning that the pollutant is simply transferred from one medium to another. This makes the spent activated carbon a hazardous waste, potentially more harmful than the original pollutant. Treatment of this contaminated carbon is complex and expensive, with a treatment cost of about $500/ton and a transport cost of about $3/mile to a

hazardous waste landfill. Finally, adsorption with activated carbon is not efficient due to its high cost and the negative environmental impact associated with the handling and treatment of contaminated carbon. For these reasons, other more efficient, environmentally friendly and economically viable ways of pollutant degradation are being investigated. [8]

1.2.1. Thiacloprid

Thiacloprid is a neonicotinoid insecticide, with a structure of cyanamide ([3-(6-chloro-3-pyridinylmethyl)-2-thiazolidinylidene]). [9]

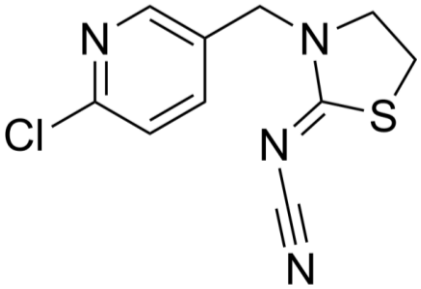

Fig 2. Chemical structure of Thiacloprid molecule. [10]

It is widely exploited in agriculture due to its high selectivity and effectiveness against some destructive crop pests, enabling the control of sucking and chewing insects on vegetables and fruits. [11, 12]

Enhanced by its strong polarity [13] that can be readily transported into aquatic environments through runoff events [14, 15], snowmelt [14], or due to wind or soil disturbances from tillage. [16]

Its high solubility in water facilitates contamination of both soil and water, posing a significant risk to aquatic organisms. [17]

Thiacloprid was experimentally proven to cause many pathological and behavioral changes in aquatic organisms [18-23], and according to its safety data sheet CAS No. 111988-49-9, it is a harmful molecule by ingestion and inhalation, may impair fertility, is suspected to cause cancer and is very toxic to aquatic organisms with long lasting effects.

1.2.2. Metoprolol

Similarly, metoprolol is a drug with a structure of 1-(iso-propylamino)-3-[4'(2-methoxyethyl)phenoxy]-2-propanol [24], which belongs to the class of pharmaceutical and personal care products (PPCPs).

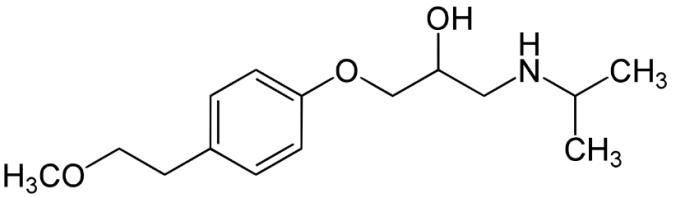

Fig 3. Chemical structure of Metoprolol molecule.[25]

Metoprolol falls within a category of medications called β-blockers. These drugs function by inhibiting the activity of specific natural substances in the body, like adrenaline, which have the potential to elevate heart rate and blood pressure. [26] The application of metoprolol is focused on the treatment of hypertension, angina (chest pain) or congestive heart failure. [27]

The use of metoprolol has increased significantly in recent years, with up to a four-fold increase compared to other similar drugs, probably due to the increased awareness of cardiovascular health management. [28, 29] By the reason, it is frequently detected in the water environment, often originating from hospitals, pharmaceutical industries or domestic sources. [30]

Metoprolol can be found in its original form, in the form of metoprolol salt (as tartrate or succinate) or in the form of metoprolol metabolites in the aquatic environment via human excretion. [31] According to the safety data sheet CAS No. 51384-51-1 (Metoprolol), CAS No. 56392-17-7 (Metoprolol tartrate) and CAS No. 098418-47-4 (Metoprolol succinate), these molecules pose a risk as they have the potential to induce skin and eye irritation, and may cause long lasting harmful effects to aquatic life.

In zebrafish embryos, the explosion of metoprolol at a specific concentration and duration has been shown to induce scoliosis and delayed growth effects. [32]

1.3. ADVANCED OXIDATION PROCESSES (AOPs)

As mentioned in the previous section, the removal of persistent organic pollutants (POPs) is in most cases not possible by conventional water treatment methods such as filtration, adsorption and sedimentation. After the application of these treatments they do not involve the destruction of the pollutant but only its passage from one medium to the other.

Therefore, the implementation of advanced technologies is resorted to, among them advanced oxidation processes (AOPs), due to their ability to induce changes in the chemical structure of organic composites. Moreover, these processes are particularly effective in the oxidation of potentially toxic by-products derived from the original composites, which could not be removed by other methods without a lengthy process.

AOPs are a set of techniques based on physicochemical processes that cause profound changes in the chemical structure of the pollutants, as in the case of organic matter removal, the objective is to achieve the mineralization of the pollutant, converting it into inorganic forms (CO_2, H_2O and halides in the case of halogenates). And depending on the technique used, the catalyst for each process can be: H_2O_2, O_3, Fe^{2+}, UV, semiconductor, energy, etc.

Removal techniques are based on the use of powerful oxidizing agents, especially hydroxyl radicals (·OH), due to their high oxidation potential (E_0=2.80 V) and their non-selective nature. This radical is therefore highly effective for the destruction of organic matter, especially non-biodegradable matter, where oxidation by conventional oxidants such as ozone, oxygen and chlorine was not possible. [33]

Fluorine is the oxidizing agent with the highest oxidation potential, but it is not used in AOPs because it is a highly toxic composite. For this reason, hydroxyl radicals (·OH) are often used in advanced oxidation processes.

The following table shows the oxidation potentials of the different strong oxidants.

Table 1. Oxidation potential of strong oxidants.[34]

Oxidizing agent	Oxidation potential [V]
Fluorine	3.03
Hydroxyl radical	**2.80**
Atomic oxygen	2.42
Ozone	2.07
Hydrogen peroxide	1.78
Perhydroxyl radical	1.70
Permanganate	1.68

This radical can be generated by various means, among which the following advanced oxidation processes stand out:

1. Ozonation: by using ozone (O_3), a powerful oxidant in the presence of water decomposes into hydroxyl radicals (·OH) which allows the degradation of pollutants. Typically used for drinking water treatment, disinfection and removal of volatile organic composites (VOCs).
2. Photolysis / Ultraviolet (UV) radiation: In water treatment, in combination with oxidants such as hydrogen peroxides, UV light directly produces hydroxyl radicals (·OH) which oxidize organic molecules. This technique has wide application in drinking water treatment, disinfection and removal of toxic chemicals.
3. Fenton process: The process uses hydrogen peroxide (H_2O_2) and iron salts (Fe^{2+}) to generate hydroxyl radicals (·OH), which are highly reactive and degrade organic pollutants. It is used in the treatment of industrial effluents, degradation of dyes and toxic composites.
4. Heterogeneous photocatalysis: This process uses photocatalysts, such as titanium dioxide (TiO_2), activated by ultraviolet (UV) light to generate hydroxyl radicals (·OH) that decompose organic pollutants. It is widely applied in wastewater treatment and in the removal of emerging pollutants, including pharmaceuticals and endocrine disruptors.

1.3.1. Heterogeneous photocatalytic degradation

As a proposal for the treatment of wastewater containing emerging pollutants such as Metoprolol and Thiacloprid, it focuses on one of the advanced oxidation processes: heterogeneous photocatalysis. This technique has the advantage of using radiation to generate reactive species (electron/hole pairs) capable of eliminating organic pollutants, thus taking advantage of an inexhaustible, clean and economical energy source.

Photocatalysis is a photochemical process that exploits light of a specific wavelength, typically ultraviolet (UV) light, in conjunction with a catalyst, in this case usually semiconductors with a defined bandgap.

This is because, in conducting materials, the bandgap is virtually non-existent or very small due to the overlapping energy bands. This allows electrons to move between bands easily and with little external energy cost. However, this same feature also facilitates the recombination of electron-hole pairs.

On the other hand, the energy of the forbidden band is relatively high in insulating materials, which significantly hinders the movement of electrons and thus the formation of electron-hole pairs.

Semiconductor materials, on the other hand, are somewhere in between: they have a higher bandgap than conductors but a lower bandgap than insulators, in the range of 1 eV to 4 eV. This means that, under the right conditions, electrons can move between bands by receiving sufficient energy, which is essential for their participation in the photocatalysis process. And to prevent recombination of electron-hole pairs in non-photoactive particles, techniques such as doping are employed. These techniques inhibit the recombination of charge carriers, which increases the photoactivity of the material.

In the process, the photocatalyst absorbs the energy provided by the photon to activate and generate electron/hole pairs. Specifically, the photon energy received by the photocatalyst must be equal to or higher than the energy of the forbidden band to promote the photo-expulsion of electrons from the valence band to the conduction band in order to generate electron/hole pairs. [35]

Each electron (e^-) that is excited into the conduction band leaves an unoccupied state in the valence band. This unoccupied state is called a hole (h^+). The simultaneous occurrence of

electrons in the conduction band and holes in the valence band results in the formation of electron/hole pairs, also known as charge carriers. [36]

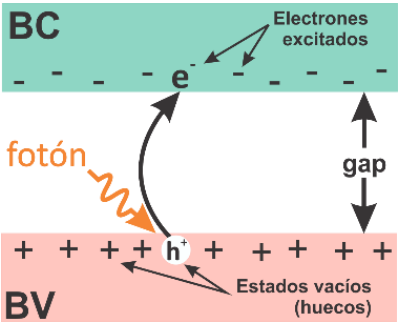

Fig 4. Energy band diagram of a semiconductor[37]

In this way, electron/hole pairs are transferred to the surface of the semiconductor particle (photocatalyst) and can participate in the redox reaction with other molecules present in the system, forming the necessary radicals that will carry out the degradation of organic molecules into inorganic forms. The reduction and oxidation reaction are shown in the figure 5.

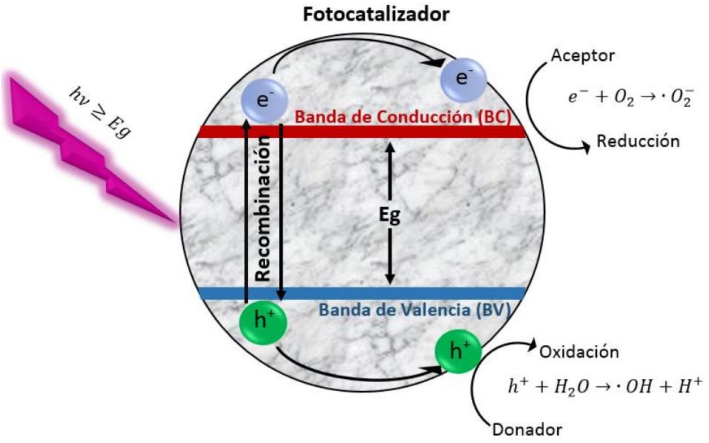

Fig 5. Heterogeneous photocatalysis process [35]

Therefore, the essential elements in the photocatalysis reaction include: the organic composite to be degraded, an oxidizing agent such as oxygen present in the air, the medium in which the reaction takes place, in this case wastewater, a photocatalyst of semiconductor material, and a light source, which can be natural (sunlight) or artificial (lamps). [38]

After the generation of the electron/hole pairs (Eq.1) the following chemical reactions take place:

$$hv + fotocatalizador \rightarrow e^- + h^+ \quad (1)$$

$$O_2 + e^- \rightarrow \cdot O_2^- \quad (2)$$

$$\cdot O_2^- + h^+ \rightarrow \cdot OOH \quad (3)$$

$$2(\cdot OOH) \rightarrow O_2 + H_2O_2 \quad (4)$$

$$H_2O_2 + \cdot O_2^- \rightarrow \cdot OH + OH^- + O_2 \quad (5)$$

$$H_2O_2 + hv \rightarrow 2 \cdot OH \quad (6)$$

In water purification treatment by heterogeneous photocatalysis, the process is generally carried out in the presence of oxygen (O_2) from the air as an oxidizing agent. In this way, O_2 accepts electrons and is reduced, forming the superoxide radical ($\cdot O_2^-$) (Eq. 2).

This superoxide radical is oxidized upon reaction with a hole (oxidizing agent) leading to the formation of the hydroperoxyl radical (·OOH) (Eq. 3), The proton (H^+) necessary for this reaction comes from the aqueous medium.

The hydroperoxyl radical is reduced to form hydrogen peroxide (H_2O_2). Likewise, hydrogen peroxide, when reacting with ($\cdot O_2^-$) (Eq. 5) and interacting with the photon energy (hv) (Eq. 6), produces hydroxyl radicals (·OH). [35, 39]

$$H_2O_{ads} + h^+ \rightarrow \cdot OH + H^+ \quad (7)$$

$$\cdot OH_{sup} + h^+ \rightarrow \cdot OH \quad (8)$$

On the other hand, oxidation of the water molecules adsorbed on the semiconductor and of the surface hydroxyls (by transferring electrons to the photogenerated holes) leads to the formation of more hydroxyl radicals (Eq. 7-8).

The formation of various types of radicals is involved in the photodegradation of organic pollutants. Among these processes, the direct oxidation of organic pollutants by interaction with

holes, the reaction with superoxide radicals and, most importantly, the reaction with hydroxyl radicals are the most important. [40]

$$Pollutant + (\cdot OH, h^+, \cdot OOH \; or \; \cdot O_2^-) \rightarrow pollutant\; degradation \quad (9)$$

The overall process of heterogeneous photocatalysis culminates in the degradation of organic pollutants into CO_2, H_2O and other components, as shown in the figure below:

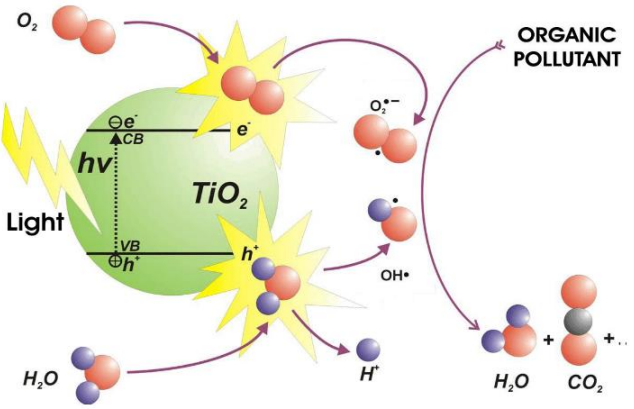

Fig 6. Overall photodegradation process using semiconductor titanium dioxide (TiO_2) [41]

1.3.1.1. Hydrozincite ($HDZn/Zn_5(CO_3)_2(OH)_6$)

Hydrozincite is a material that can be formed either naturally or synthetically and is characterized by a gap band of 5.2 eV. [42]

In terms of catalytic degradation, a study has shown that hydrozincite exhibits 2.31 times higher photocatalytic activity than ZnCO3 in the degradation of methylene blue by ultraviolet light irradiation. [43]

In a study of the synthesis and characterisation of ZrO_2 (Zirconium Oxide) / $Zn_5(CO_3)_2(OH)_6$ (HDZn) composite materials, where HDZn acts as the supporting catalyst, the results obtained in the photocatalytic reaction showed that the addition of ZrO_2 to $Zn_5(CO_3)_2(OH)_6$ significantly increased the photoactivity of the material.

In particular, the sample with 8% in mol of ZrO_2 (ZnZr - 8.0%) presented the best photodegradation and mineralization rates, thanks to an increase in the specific surface area and

improved charge transfer at the composite interface. XPS (photoelectron spectroscopy) studies indicated that the oxygen vacancies induced by ZrO_2 favor the photodegradation of organic molecules through direct hole attack.

These findings suggest that the ZnZr composite system is a promising option for the photodegradation of persistent organic pollutants, due to its reduced cost, high stability and low toxicity. [44]

1.4. HYDROCHAR

Recently, the demand for carbon materials, such as carbon fibres, structural graphite, graphene, carbon nanotubes and carbon foams, has progressively increased due to their wide application in various sectors, such as aerospace, automotive and construction. The production of these materials involves high costs as well as the consumption of non-renewable petroleum precursors, which has led to significant environmental concerns. Consequently, the demand for the production of carbon materials using renewable sources has increased at an annual rate of 10%. [45]

Hydrochar is characterized as a non-toxic, high-carbon solid material generated from biomass, which is recognized as a sustainable energy source. Biomass sources include agricultural waste, forestry waste, municipal solid waste and algae waste. [46, 47]

Hydrochar is recognized as an effective alternative adsorbent for the removal of organic dyes from wastewater due to its good porous structure, well-developed surface area and substantial oxygen-containing functional groups (hydroxyl, phenolic, carbonyl or carboxylic) on the surface. [48]

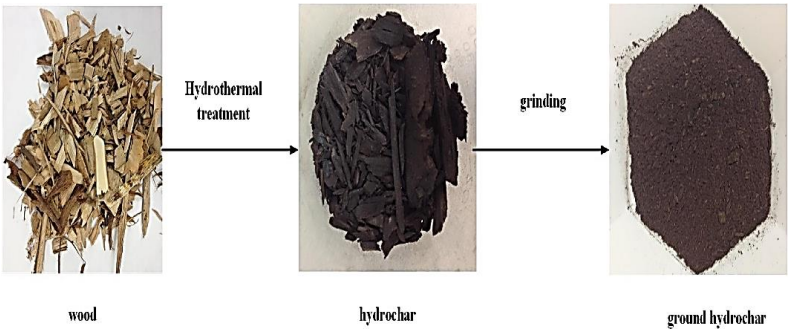

Fig 7. Hydrochar produced from wood sample [49]

1.4.1. Hydrothermal Carbonization (HTC)

In recent years, the hydrothermal carbonization process (HTC) has emerged as an alternative method to process biomass into value-added products. Where waste biomass can be directly converted into a carbon-rich material by HTC at moderate temperatures (180-350°C), autogenous pressures and in the presence of water for several hours. In contrast to pyrolysis, HTC is generally considered more environmentally friendly, suitable and economical due to the elimination of the drying step and requires a lower treatment temperature than pyrolysis. To differentiate from the solid product generated by pyrolysis (biochar), it is referred to as hydrochar. [45, 48, 49]

As the process temperature increases, the biopolymer bonds are broken while water molecules penetrate through the porous structure of the solid, decomposing the biomass by dissolving intermediate products through polymerization and decomposition similar to pyrolysis. On the other hand, in the case of pyrolysis for biochar synthesis (without the presence of water), the treatment is required to be carried out in a higher temperature range, varying between 350 and 700 ºC, and in an oxygen-limited environment, which implies a higher energy consumption compared to hydrochar synthesis. [50-53]

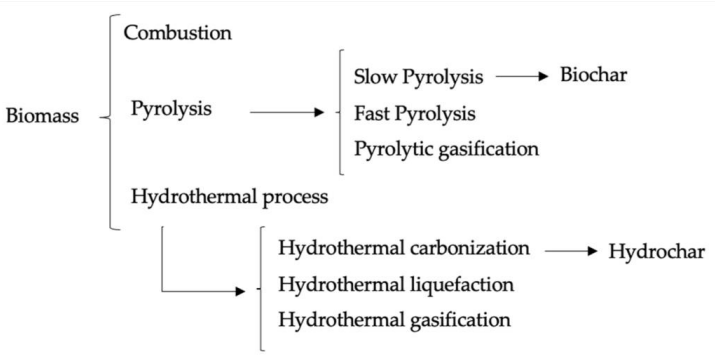

Fig 8. Conversion pathways from biomass to bio/hydrochar.[45]

Both materials can be used as a basis for other functional materials while promoting sustainability and circular economy principles, due to the abundance, renewability and low cost of their raw materials. [54, 55]

However, hydrochar prepared by hydrothermal carbonization (HTC) has a low surface area and strong binding sites that limit its adsorption capacity. Therefore, modification or activation of hydrochar is imperative to increase its adsorption capacity by incorporating chemicals, such as

phosphoric acid. The addition of acids has been reported to catalyze the hydrolysis reaction, which enhances the active surface area and functional groups of hydrochar. [48]

1.4.2. Application of hydrochar in adsorption

Hydrochar's various applications highlight its use in environmental remediation, such as water purification and soil remediation, as well as its gas adsorption capacity and its application in power generation, among other applications.

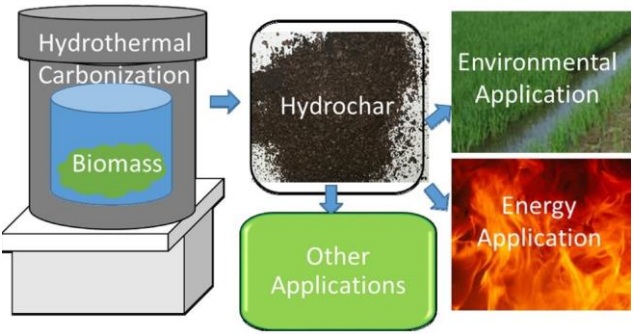

Fig 9. A summary of major applications of hydrochar [49]

In recent times, there has been a remarkable increase in research on the application of hydrochar for environmental remediation, driven by the growing concern for environmental problems in contemporary times. [56]

Adsorption with active carbons and hydrochar present significant differences in terms of cost and environmental impact. While hydrochar tends to be more economical due to its less intensive production process and the use of low-cost raw materials, it also generates less environmental impacts. This is because it consumes less energy for its production and is mainly made from renewable sources (biomass waste).

The use of hydrochar as an adsorbent for pollutant removal is highlighted by the crucial role of surface chemistry (including total pore volume, specific surface area, functionality and microporosity) in adsorption efficiency. These characteristics depend on the temperature and reaction duration applied during hydrothermal carbonization (HTC). [57]

Hydrochar has shown great potential to adsorb a wide range of pollutants, including organic dyes, herbicides/pesticides, heavy metals, pharmaceuticals and CO_2, both with and without chemical or physical modification. In a study on hydrochar synthesis and adsorption of dye-contaminated water, glucose was used as raw material, obtaining 100% removal efficiency (5.3 µmol/g) for the cationic dye (methylene blue) and anionic dyes (organic methylene and reactive yellow-II). In addition, simultaneous adsorption of both dyes was achieved. Regarding heavy metals, hydrochar has shown efficiency in the adsorption of zinc (Zn^{2+}), copper (Cu^{2+}) and lead (Pb^{2+}) ions, all of which are harmful to human health and the environment due to their toxicity and lack of biodegradability. [56]

It is crucial to note that hydrochar generated from different biomass sources exhibits different characteristics, resulting in variations in its adsorption capacity with respect to the same pollutant. These differences may be influenced by the synthesis conditions during hydrothermal carbonization. Therefore, the choice of biomass and processing conditions are determining factors in the effectiveness of hydrochar as an adsorbent for pollutant removal. [56]

That said, the efficiency of hydrochar in adsorption is subject to several factors, including the type of contaminant to be treated, the conditions of the solution and the specific characteristics of the hydrochar employed. Therefore, the use of hydrochar for pollutant removal by adsorption does not always ensure total effectiveness. [57]

On the other hand, a limitation of adsorption is that, after the process of adsorbing the contaminants onto the hydrochar, the hydrochar becomes contaminated and saturated on its surface, requiring regeneration or replacement. Further regeneration may involve the use of chemicals or thermal processes, leading to additional environmental impacts. As mentioned in previous sections, this method transfers the contaminant from one medium to another.

1.4.3. Application of hydrochar in photocatalysis

So far, the scientific literature has documented a paucity of studies on the application of hydrochar in photocatalysis. However, among the few studies carried out, promising results have been identified.

A study on the combination of the photocatalyst Fe_3O_4/BiOBr@HC20% (HC mass ratios 20%), where HC has been used as a support catalyst (by HC microspheres), showed a 100% removal of the analgesic carbamazepine (CBZ) and 67.41% of total organic carbon (TOC) in 40

minutes, under LED-visible light irradiation. This result outperformed other photocatalysts, because the narrow band gap (2.02 eV) of the combined photocatalyst enhanced the absorption of visible light. In addition, hydrochar, with its abundant oxygen functional groups on the surface, provided more active oxygen species, such as $\cdot O_2^-$ and ·OH, acting as an electron bridge to promote electron transfer between Fe_3O_4 and BiOBr.

According to this study, the potential of this system has been demonstrated in the efficient degradation of refractory pollutants and in the evaluation of photocatalysts composed of a semiconductor and a non-semiconductor material in photocatalytic degradation.

Furthermore, it was observed that the Fe_3O_4/BiOBr@HC composite catalysts maintain excellent reusability and stability over five experimental cycles. [58]

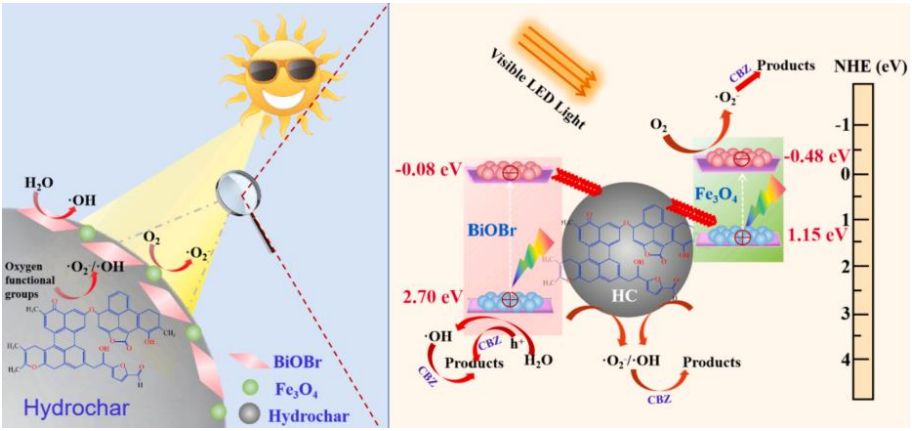

Fig 10. Proposed photocatalytic mechanism of Fe3O4/BiOBr@HC20% towards CBZ degradation. [58]

Compared to adsorption, photocatalysis provides a more complete degradation of pollutants, leading to a decrease in waste generation. During the photocatalytic process, pollutants could be transformed into less harmful products or even harmless composites, in contrast to adsorption, which can only retain them on the surface.

Moreover, the photocatalyst can be reused multiple times with lower costs compared to adsorption, suggesting a promising future for its application.

2. OBJECTIVES

The main objective of this work is to evaluate the viability of hydrochar/Zn composites as photocatalysts in the degradation of organic pollutants through heterogeneous photocatalytic processes. To achieve this objective, previous studies have been carried out on the materials involved in the experimental work. Hydrochar (HC) has shown good results in adsorption and hydrozincite (HDZn) is known to show efficiency in photocatalysis when combined with other oxides.

Therefore, it is proposed to synthesize a photocatalyst based on the combination of HC and HDZn, which aims to evaluate the individual performance of HC in photocatalysis and its effectiveness after combination with other materials in different ratios. For comparative purposes, the combination of HC with zinc nitrate (ZnN_2O_6) is also evaluated.

The experimental work covers the following specific objectives:

- Synthetize HC (hydrochar) from biomass residues from vine shoots and HDZn or $Zn_5(CO_3)_2(OH)_6$ (hydrozincite).
- Form HC/HDZn and HC/ ZnN_2O_6 composites in different weight percentages of Zn.
- Analyze the efficiency of HC individually in photodegradation.
- Evaluate the efficiency of HC/HDZn and HC/ZnN_2O_6 composites in the degradation of selected organic pollutants (Metoprolol and Thiacloprid).
- Determine the efficiency of HC (synthesized from vine shoots) in the adsorption of selected pollutants.
- Identify the composite with the best performance in the photocatalytic degradation of each pollutant, for reuse in multiple degradation cycles.

3. EXPERIMENTAL

3.1. SYNTHESIS OF MATERIALS

3.1.1. Synthesis of HDZn

The synthesis of HDZn is carried out by the methods of chemical co-precipitation and thermal hydrolysis of urea.

In a round bottom flask, 250 ml of distilled water, 3 ml of nitric acid are added sequentially. As this method of synthesis requires the use of a precipitating agent in excess, urea is used in a 3:1 ratio of nitrate: urea ions. This process is carried out while a magnetic core is inserted into the flask to facilitate the stirring of the solution. [44]

The solution is placed in a magnetic stirrer with a heater and kept at a temperature of 150°C for a period of 36 hours. During this time, stirring is maintained at 800 rpm. [44]

After completion of the reaction, white precipitates (HDZn with nitrate) are detected in the reaction vessel. These precipitates are filtered (under vacuum) and washed with copious amounts of boiling water to remove the nitrate ions from the zinc nitrate. Filtering is continued until the rinse water reaches a neutral pH.

The need to remove nitrates before exposing the precipitates to high temperatures in the flask is due to the propensity of nitrates to undergo thermal decomposition when heated. This decomposition can lead to dangerous gases, explosions, or fires if not handled properly. Therefore, thorough washing of the precipitates is aimed at preventing these potential hazards during the heating process in the muffle.

After placing the HDZn precipitate in the flask, it is kept at a temperature of 100 ºC for a period of 24 hours, which allows its proper preparation.

Once the procedures described above have been completed, the desired final product is obtained: HDZn, characterized by its white powder form, labelled as HDZn in a container.

3.1.2. Synthesis of HC

In the hydrothermal carbonization process (HTC), the transformation is carried out in a pressure vessel, where biomass derived from vine shoots, previously ground, is used as the main raw material.

Previous studies have been carried out on the synthesis of HC with and without acidification using nitric acid and phosphoric acid in different molar concentrations, obtaining better results when synthesized with a 2M solution of phosphoric acid. The presence of phosphoric acid can integrate electronegative functional groups on the surface of the catalyst, improving its activity compared to HC synthesized with water alone. This will be further analyzed in future works, where the characterization of all the synthesized materials will be deepened.

That said, 50 ml of an aqueous phosphoric acid solution with a concentration of 2 M is prepared in this work. [48]

To determine the amount of concentrated acid to be removed for dilution to the desired concentration:

$$2\ \frac{mol}{L} \times 98\ \frac{g}{mol} \times \frac{1\ L}{1{,}7\ kg} \times \frac{1\ kg}{1000\ g} \times 50\ ml = 5{,}8\ ml\ Phosphoric\ acid\ conc. \qquad (10)$$

Once the dilute acid solution has been prepared, it is introduced into the hydrothermal autoclaved Teflon reactor, together with the addition of 5 g of biomass. In addition, a magnetic core is incorporated to facilitate homogeneous stirring of the reactor contents.

The reaction is initiated by hermetically sealing the reactor and placing it in the stirrer with heater, setting a temperature of 250 ºC and a stirring speed of 110 rpm. This process is carried out over a period of 4 hours.

After completion of the reaction, the system is allowed to cool down to room temperature through exposure to ambient air.

Through the vacuum filtration process, the separation of the oil from the hydrochar is carried out, using 3 liters of distilled water for rinsing. Subsequently, pure hydrochar is obtained as the final product. This hydrochar is further dried in the muffle at 100 ºC for a period of 24 hours.

In this way, the synthesis of hydrochar is achieved from the biomass derived from vine shoots, with the final product being labelled as HC.

3.1.3. Synthesis of HC-HDZn

In the synthesis process of the HC-HDZn composites, a constant amount of HC, in this case 5 grams, is incorporated together with a variable proportion of HDZn ranging from 5% to 15% by weight with respect to HC.

In case of synthesis of the HC-HDZn5% composite, a magnetic core is introduced into the hydrothermal autoclaved Teflon reactor together with:

- 5 g of synthesized HC
- 5% by weight equals 0.25 g of HDZn
- 50 ml of phosphoric acid 2 M

The same procedure used in the HC synthesis is performed, where the reactor is hermetically sealed and placed in the stirrer with heater. A temperature of 300 °C and a stirring speed of 110 rpm is set. This process is maintained for a continuous period of 4 hours.

Once the reaction is finished, the system is cooled down before the washing and vacuum filtration process. Subsequently, the product undergoes the drying process in the muffle, following the same steps detailed in the HC synthesis section.

In this way, the synthesis of the composite HC-HDZn of different proportions is achieved, with the final product labelled as HC-HDZn X%, where X represents the percentage by weight.

3.1.4. Synthesis of HC-ZnN_2O_6

As described in the objectives section, the synthesis of HC-ZnNN2O6 is carried out in order to make a comparison with the case of HC-HDZn. HC-ZnN2O6 is also synthesized in variable proportion of ZnN2O6, ranging from 5% to 15% by weight with respect to HC.

In case of synthesis of the composite HC-ZnN2O6 (10%, a magnetic core is introduced into the hydrothermal autoclaved Teflon reactor together with:

- 5 g of synthesized HC
- 10% by weight is equivalent to 0.5 g of ZnN2O6
- 50 ml of phosphoric acid 2 M

The procedure is carried out analogously to the one used in HC synthesis. Initially, the reactor is hermetically sealed and placed in the stirrer with heater, setting a temperature of 300 ºC and a stirring speed of 110 rpm. This process is prolonged for a period of 4 hours.

At the end of the reaction, the system is cooled down before starting the washing and vacuum filtration process. Subsequently, the resulting product is subjected to the drying process in the muffle, meticulously following the same steps described in the HC synthesis section.

In this way, the synthesis of the composite HC-ZnN2O6 is achieved, varying the proportions as required.

The final product is labelled as HC-ZnNN2O6 X%, where X represents the percentage by weight.

3.2. EXPERIMENTAL DESIGN

As detailed in the objectives section, the photodegradation of two types of pollutants, Metoprolol and Thiacloprid, will be carried out. These pollutants will be treated using previously synthesized photocatalysts, as shown in the following tables.

For each pollutant, the heterogeneous photocatalysis process is performed seven times, using the different ratios of photocatalysts prepared in each reaction. In total, 14 photocatalytic reactions will be carried out.

The conditions kept constant include a stirring speed of 500 rpm without heat application, reaction at room temperature, an identical duration of the reaction process, as well as air injection and exposure to ultraviolet (UV) radiation in the system.

Table 2. Proposed Photocatalytic Reactions for Contaminant Degradation.

Metoprolol Reactions	Photocatalyst	**Thiacloprid** Reactions	Photocatalyst
R1	HC	R8	HC
R2	HC-HDZn5%	R9	HC-HDZn5%
R3	HC-HDZn10%	R10	HC-HDZn10%
R4	HC-HDZn15%	R11	HC-HDZn15%
R5	HC-$ZnN_2O_6$5%	R12	HC-$ZnN_2O_6$5%
R6	HC-$ZnN_2O_6$10%	R13	HC-$ZnN_2O_6$10%
R7	HC-$ZnN_2O_6$15%	R14	HC-$ZnN_2O_6$15%

For each reaction, a total process of 4 hours is carried out, involving a total of 10 samples.

First, the initial contaminant sample is taken (1 sample). Then, the adsorption of contaminants by the composite is carried out for 1 hour (1 sample taken). Subsequently, samples of the aqueous medium are taken every 15 minutes until one hour is completed (4 samples taken). Thereafter, a sample is collected every half hour until a total photocatalysis duration of 3 hours is reached (4 samples taken).

After identifying the photocatalyst with the most promising degradation performance, reuse experiments were carried out in degradation cycles to evaluate its continuous capability. These experiments involved determining the degradation efficiency of the compound after multiple reuse cycles, each lasting three hours.

Three reuse cycles of the photocatalyst are suggested for each pollutant evaluated, where "OP" represents the optimal photocatalyst.

Table 3. Cycles of reuse of optimal photocatalysts.

Cycles of reuse	**Metoprolol**	**Thiacloprid**
C1	OP_M	OP_T
C2	OP_M	OP_T
C3	OP_M	OP_T

3.3. EXPERIMENTAL PROCEDURE

3.3.1. Process of photodegradation

400 ml of water contaminated with Metoprolol at a concentration of 5 ppm is prepared, and the same procedure is carried out with Thiacloprid. Once the solution is prepared, an initial sample of the contaminated water is taken in 1.5 ml vials.

1 g/L of photocatalyst, which in this case is 400 mg of the photocatalyst corresponding to the reactor, is introduced together with the magnetic core and 400 ml of contaminated water with a concentration of 5 ppm.

The reactor used to carry out the photocatalytic reaction is a 500 ml batch reactor, covered with aluminium foil to prevent the entry of external light and to maintain controlled conditions during the photodegradation reaction.

A UV lamp with a wavelength of 254 nm and an air inlet are introduced. The function of the air pump is to inject oxygen (O2) into the aqueous medium and to benefit the production of superoxide radicals.

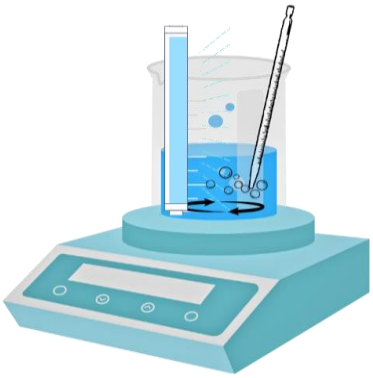

Fig 11. Experimental device of heterogeneous photocatalytic reaction.

Once everything is prepared, the experiment is started by turning on the stirrer at 500 rpm with the air pump. It is important to note that the UV lamp is not activated until one hour into the adsorption phase. Once this phase is completed, the second sample is taken for analysis.

After one hour of adsorption, the UV lamp is activated, keeping all experimental conditions constant as before.

During the first hour of the photocatalysis phase, samples are taken every 15 minutes. From the second hour until the end of the phase, samples are taken every 30 minutes.

At the end of a reaction, the photocatalyst is filtered under vacuum and stored for future cyclic reactions.

A total of 14 reactions are carried out; each pollutant is treated 7 times, each time using the photocatalysts proposed in the experimental design.

3.3.2. Reusability cycles in photocatalytic degradation

Once the composites that achieve the highest degradation of pollutants have been determined, 3 reuse cycles are carried out to evaluate their continued degradation capacity and stability.

A total of 6 cycles are carried out, distributed equally with 3 cycles for each pollutant.

In the first cycle, 400 ml of contaminated water with a concentration of 5 ppm is added to the reactor, together with 0.4 g of the optimum composite. The reaction is carried out for 3 hours, without the need to take intermediate samples, and only one sample is taken at the end of the degradation cycle.

At the end of the first cycle, only the photocatalyst used is filtered under vacuum, without the need to rinse with distilled water. The filter paper, together with the photocatalyst, is placed in the muffle for drying and subsequent use after 24 hours.

For the second cycle, the remaining photocatalyst powders after their use in degradation, filtration, and drying are collected and removed from the filter paper. It is important to note that there may be mass losses of the photocatalyst during this process.

With the remaining mass of the photocatalyst, a quantity of contaminated water is added, maintaining the initial catalyst concentration of 1 g/l. For example, if 380 mg of photocatalyst remain, 380 ml of contaminated water will be introduced to perform the degradation. The sample of the second cycle is taken at the end.

This procedure is repeated in the same way for the third cycle.

In this way, 6 samples are obtained from the cycle to be analyzed by HPLC (High-Performance Liquid Chromatography), which is a laboratory technique used to separate, identify, and quantify components of a liquid sample.

4. RESULTS AND DISCUSSION

4.1. CALIBRATION

A calibration is carried out to establish the correspondence between the area of the peaks obtained by high performance liquid chromatography (HPLC), using the UV detector (Agilent Model 1260 Infinity), and the concentrations of metoprolol and thiacloprid expressed in parts per million (ppm). Through this procedure, the calibration curves illustrated in figures 12 and 13 are generated.

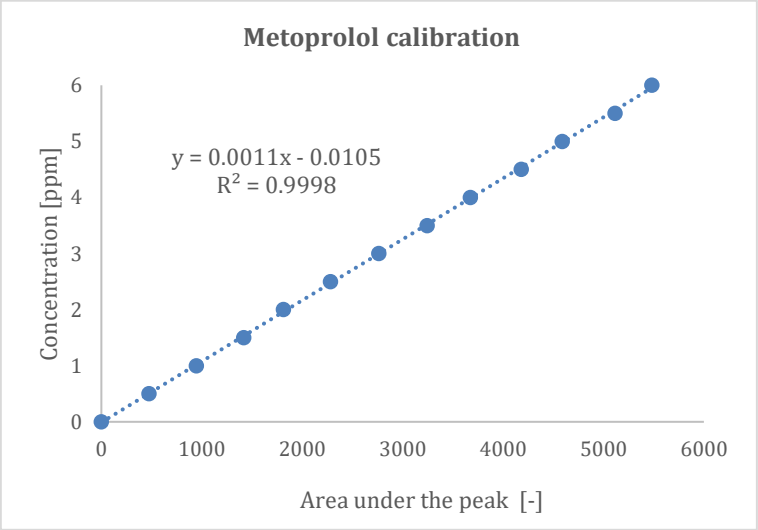

Fig 12. Variation of metoprolol concentration as a function of area under the peak.

The calibration equation obtained by linear regression is as follows:

$$\boldsymbol{C_M}\ [\text{ppm}] = (1.0880 \pm 0.005) \times 10^{-3} \times \mathbf{Area} + (-1.0529 \pm 1.6862) \times 10^{-2} \quad (11)$$

However, in this case, it is observed that the constant term in the equation is not significant. The standard deviation of the constant term is larger than the absolute value of the constant term itself.

This implies that the constant term can be excluded as it is not relevant for predicting metoprolol concentration.

$$|-1.0529| < 1.6862 \quad (12)$$

Finally, this equation of the calibration curve is obtained:

$$\boldsymbol{C_M}\ [\text{ppm}] = (1.0880 \pm 0.005) \times 10^{-3} \times \mathbf{Area} \quad (13)$$

Similarly, the thiacloprid calibration curve is obtained.

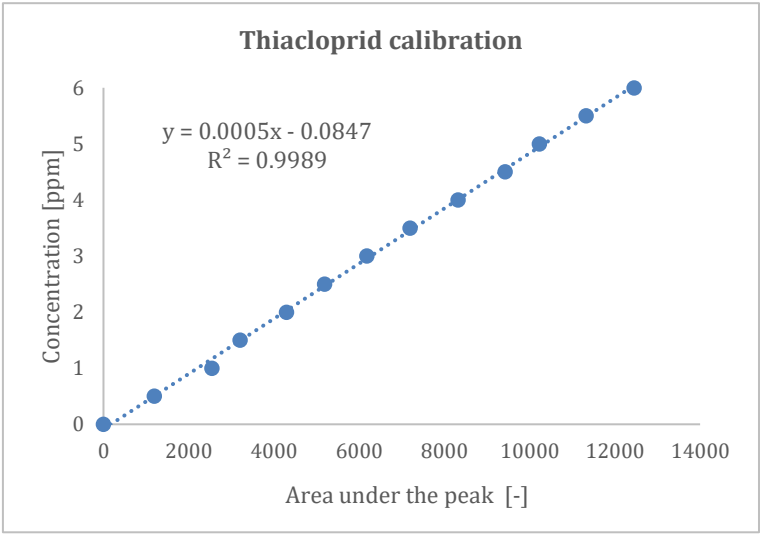

Fig 13. Variation of thiacloprid concentration as a function of area under the peak.

$$\boldsymbol{C_T}\ [\text{ppm}] = (4.9180 \pm 0.0484) \times 10^{-4} \times \mathbf{Area} + (-8.4729 \pm 3.5474) \times 10^{-2} \quad (14)$$

In this case, even though the value of the constant term is greater than the error, as it represents approximately 40% of the error, it is decided to simplify the model by excluding this term.

$$|-8.4729| > 3.5474 \quad (15)$$

Finally, the equation of the thiacloprid concentration curve is as follows:

$$\boldsymbol{C_T}\ [\text{ppm}] = (4.9180 \pm 0.0484) \times 10^{-4} \times \mathbf{Area} \quad (16)$$

4.2. EVALUATION OF THE EFFECTIVENESS OF COMPOSITES IN THE ADSORPTION PROCESS

Table 4. Result of the variation of metoprolol concentration in the adsorption process.

	HC	**HC-HDZn 5%**	**HC-HDZn 10%**	**HC-HDZn 15%**	**HC-ZnN_2O_6 5%**	**HC-ZnN_2O_6 10%**	**HC-ZnN_2O_6 15%**
Time [min]	C_M [ppm]	C_M [ppm]	C_M [ppm]	C_M [ppm]	C_M [ppm]	C_M [ppm]	C_M [ppm]
0	5.0070	5.0101	5.0090	5.0091	5.0088	5.0081	5.0110
60	5.0058	5.0096	5.0080	5.0080	5.0088	5.0088	5.0099

Table 5. Result of the variation of thiacloprid concentration in the adsorption process.

	HC	**HC-HDZn 5%**	**HC-HDZn 10%**	**HC-HDZn 15%**	**HC-ZnN_2O_6 5%**	**HC-ZnN_2O_6 10%**	**HC-ZnN_2O_6 15%**
Time [min]	C_T [ppm]	C_T [ppm]	C_T [ppm]	C_T [ppm]	C_T [ppm]	C_T [ppm]	C_T [ppm]
0	5.0826	5.0338	5.0715	5.0386	5.0343	5.0720	5.0390
60	5.0337	5.0826	5.0731	5.0774	5.0288	5.0736	5.0779

Table 4 and 5 shows that the HC composites with organic matter origin vine shoot is not effective in adsorbing the pollutants metoprolol and thiacloprid.

The concentration of the contaminants remained practically unchanged during the one-hour adsorption period, suggesting a low affinity between the HC composites and the contaminants.

Occasional increases in concentration were observed in table 5 in some cases, possibly due to experimental errors. These errors could have occurred when extracting the samples, as the

residual presence of the previous sample on the sample holder filter could have slightly affected the results of the next sample.

Previous studies have shown a significant improvement in adsorption capacity by activating HC with phosphoric acid during the synthesis process. In the specific case of the use of HC from vine shoot organic matter, this aspect was not explored in this study.

A possible explanation for the inefficiency of HC in adsorption could be the low specific surface area and porosity of HC, which limit the number of sites available for adsorption. HC was synthesized under moderate temperature conditions and with a relatively short process time, which could be the reason for its low specific surface area and limited porosity.

Further research on the structure of this type of HC, derived from grapevine shoots, is required to perform more comprehensive analyses and to explain why it is not effective in adsorption, unlike other organic materials.

Therefore, it is suggested that future research should focus on the modification of HC, by increasing the synthesis temperature and prolonging the synthesis time, to investigate whether these two factors could improve its efficiency in adsorbing the aforementioned pollutants. Furthermore, it would be relevant to explore the combination of HC with other adsorbent materials, which could lead to more promising results.

It is concluded that this type of synthesized HC does not prove to be suitable for the adsorption of the pollutants metoprolol and thiacloprid in wastewater treatment applications.

4.3. EFFECTIVENESS OF INDIVIDUAL HC ON PHOTODEGRADATION

Table 6. Variation of pollutant concentration and percentage of degradation in photodegradation applying individual HC.

Time [min]	C_M [ppm]	η_M [%]	C_T [ppm]	η_T [%]
0	5.0058	0.00%	5.0337	0.00%
15	4.8111	3.89%	4.8828	3.00%
30	4.5083	9.94%	4.7829	4.98%
45	4.3116	13.87%	4.6830	6.97%
60	4.2091	15.92%	4.5831	8.95%
90	4.1090	17.92%	4.4832	10.94%
120	4.0589	18.92%	4.3833	12.92%
150	4.0087	19.92%	4.2834	14.91%
180	4.0091	19.91%	4.1835	16.89%

Where η represents the photodegradation efficiency, C_M denotes the concentration of metoprolol, and C_T denotes the concentration of thiacloprid.

In the study of the photodegradation of pollutants using individual HC, the concentration after the adsorption process has been considered to be the initial concentration for the subsequent photocatalysis. This approach has been adopted because it more accurately reflects the state of the system just before the start of photocatalysis, which was carried out in the same reactor together with adsorption.

As shown in the table above, the concentration of both pollutants was reduced from approximately 5 ppm to around 4 ppm within three hours.

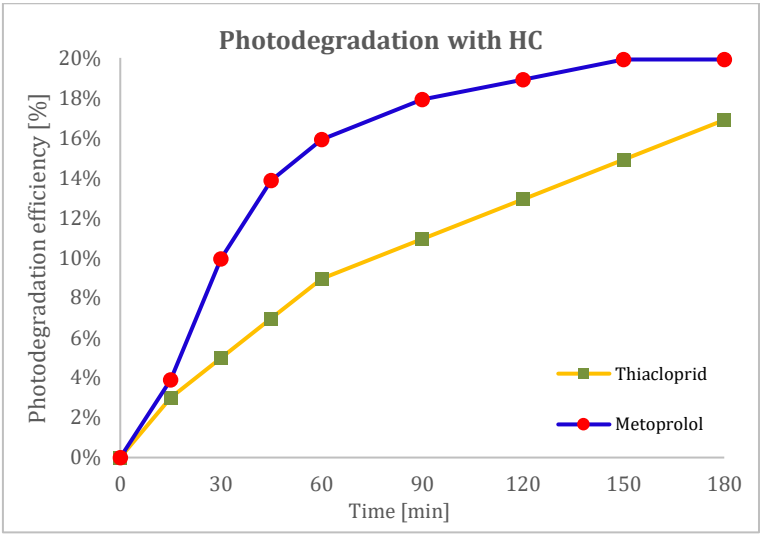

Fig 14. The relationship between the photodegradation efficiency of pollutants and the illumination time using HC as photocatalyst.

As illustrated in figure 14, during the photodegradation of the pollutants metoprolol and thiacloprid under identical reaction conditions (agitation, aeration system and exposure to UV light for 3 hours), it has been observed that HC individually has shown a faster and more efficient degradation in metoprolol compared to thiacloprid. The metoprolol curve rises rapidly, reaching 19.91% photodegradation efficiency. In the case of thiacloprid, a slower degradation occurs, reaching an efficiency of 16.89%, which is slightly lower compared to the efficiency obtained for metoprolol.

However, metoprolol degradation shows a stabilization trend between 150 and 180 minutes, with degradation percentages of 19.92% and 19.91% respectively. This slight difference may be due to experimental errors during sample sampling. It is inferred that the degradation of metoprolol using HC has reached its maximum efficiency. In contrast, thiacloprid shows a slower degradation trend with no signs of stabilization, suggesting that photodegradation may continue if exposure time is prolonged.

These results demonstrate that HC individually possesses a significant capacity for pollutant removal by the heterogeneous photocatalytic process. This efficiency significantly exceeds its adsorption capacity, which has been shown to be negligible.

A possible explanation for the performance of individually modified HC as an insulating material, with an energy band of 4.6 eV according to a study carried out by the research group (Appendix 2), in photodegradation may be due to the intervention of the functional groups introduced by the phosphoric acid.

When the photocatalyst receives UV light energy, the electrons are excited from the valence band without reaching the conduction band due to their high energy gap. Functional groups can act as surface traps for electrons and holes, facilitating the separation of electron-hole pairs and reducing their recombination. In addition, they promote charge transfer towards radical formation or directly towards the oxidation of pollutants. In this way, they contribute significantly to the degradation of pollutants, significantly improving the efficiency of the photocatalytic process.

Compared to the most investigated photocatalyst, TiO_2, which showed a metoprolol degradation of 48% after 180 minutes of treatment, pure HC achieved 19.91%. Although this result is lower, it is important to note that TiO_2 is considerably more expensive. HC, on the other hand, represents a sustainable, environmentally friendly and economical material in the process of study and development. Achieving a degradation of 19.91% is encouraging and underlines a promising potential for future improvements. [59]

The use of HC in individual water treatment applications offers significant advantages in terms of cost and sustainability. This material, known for its affordability and eco-friendliness by reusing waste, is positioned as a viable option for large-scale applications.

4.4. ANALYSIS OF METOPROLOL PERCENTAGE DEGRADATION

Table 7. Degradation percentage variation in photodegradation of metoprolol.

	HC	HC-HDZn 5%	HC-HDZn 10%	HC-HDZn 15%	HC-ZnN_2O_6 5%	HC-ZnN_2O_6 10%	HC-ZnN_2O_6 15%
Time [min]	η_M [%]	η_M [%]	η_M [%]	η_M [%]	η_M [%]	η_M [%]	η_M [%]
0	0.00%	0.00%	0.00%	0.00%	0.00%	0.00%	0.00%
15	3.89%	10.01%	19.95%	3.93%	6.00%	8.00%	7.02%
30	9.94%	29.95%	41.87%	13.91%	11.97%	13.97%	12.99%
45	13.87%	43.91%	61.86%	19.90%	15.96%	17.96%	16.98%
60	15.92%	49.90%	79.83%	25.90%	17.96%	19.96%	18.98%
90	17.92%	55.90%	93.80%	33.88%	19.96%	21.97%	22.00%
120	18.92%	58.89%	97.80%	37.90%	20.96%	22.96%	23.07%
150	19.92%	59.91%	99.80%	39.88%	21.92%	23.96%	23.00%
180	19.91%	59.90%	**99.82%**	39.88%	21.96%	23.96%	22.99%

Table 7 presents the results of the degradation of metoprolol using various previously synthesized composites. The photocatalyst with the highest photocatalytic activity, HC-HDZn 10%, achieved a degradation rate of 99.82% in 180 minutes. In contrast, HC alone only achieved 19.91% degradation, which represents 79.91% less than HC-HDZn 10%, showing a significant improvement in the efficiency of the photocatalyst.

According to the study carried out by the research group (Appendix 2), it was determined that the 10% HC-HDZn has a gap band energy of 3.2 eV, lower than the individual HC, which has an energy of 4.6 eV.

The higher efficiency of the 10% HC-HDZn can be attributed to this reduction of the band gap energy through the combination of materials, which favors photocatalytic degradation by facilitating the formation of electron-hole pairs and, subsequently, the formation of radicals and mineralization of the organic pollutant.

In the case of HC-ZnN2O6, the best performance was obtained with HC-ZnN2O6 at 10%. However, compared to the optimum HC-HDZn 10%, this performance is 75.86 % lower.

The combination of HC with ZnN_2O_6 did not result in a significant increase in degradation performance, increasing the degradation percentage only from 19.91% to 23.96%, which represents an increase of only 4.05%.

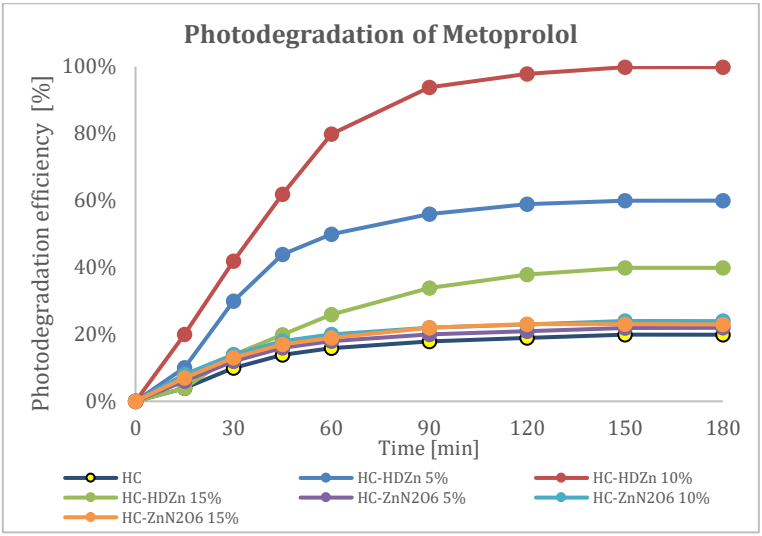

Fig 15. The relationship between the photodegradation efficiency of metoprolol and the illumination time.

The figure 15 shows that the degradation efficiency of the 10% HC-HDZn shows a faster degradation trend compared to the other materials. It is noted that in the degradation of metoprolol from HC photocatalysts or HC/Zn composites all tend to stabilize after 90 minutes, suggesting that the process has reached its maximum efficiency within 3 hours of reaction.

The three composites that have shown the highest degradation capacity in the experiment are the HC-HDZn composites, with the 10% by weight being the most efficient, followed by the 5% and in third place the 15%.

This fact implies that there is no direct relationship between increasing the percentage of HDZn and the improvement in degradation. Characterization studies, morphology and structure analysis of the material will be required to justify this phenomenon and to understand why the 10% HDZn composite shows a higher efficiency compared to the others.

4.5. ANALYSIS OF THIACLOPRID PERCENTAGE DEGRADATION

Table 8. Degradation percentage variation in photodegradation of thiacloprid.

	HC	**HC-HDZn 5%**	**HC-HDZn 10%**	**HC-HDZn 15%**	**HC-ZnN_2O_6 5%**	**HC-ZnN_2O_6 10%**	**HC-ZnN_2O_6 15%**
Time [min]	η_T [%]	η_T [%]	η_T [%]	η_T [%]	η_T [%]	η_T [%]	η_T [%]
0	0.00%	0.00%	0.00%	0.00%	0.00%	0.00%	0.00%
15	3.00%	5.90%	13.60%	3.83%	2.91%	4.75%	4.44%
30	4.98%	15.72%	27.38%	9.73%	4.63%	6.92%	6.63%
45	6.97%	23.58%	39.19%	15.64%	6.88%	8.88%	8.57%
60	8.95%	29.48%	49.04%	19.57%	8.86%	10.85%	10.54%
90	10.94%	39.31%	62.82%	25.47%	10.85%	13.60%	13.69%
120	12.92%	47.17%	72.67%	31.38%	12.83%	15.65%	15.65%
150	14.91%	53.07%	86.45%	35.31%	14.82%	18.53%	17.62%
180	16.89%	58.96%	**98.27%**	39.25%	16.82%	20.49%	19.59%

Table 8 presents the results of thiacloprid degradation of the different composites.

A similar phenomenon to metoprolol is observed; the optimal photocatalyst is still the HC-HDZn 10%, reaching a maximum degradation percentage of 98.27% in 180 minutes. Compared to the single HC, which achieved 16.89%, the degradation efficiency has been increased by 81.38%. This shows that the HC-HDZn composites have significantly increased the efficiency of the photocatalyst in the degradation of both pollutants.

As was the case for metoprolol degradation, the 10% HC-ZnN2O6 achieved the highest degradation among the HC-ZnN2O6 composites, reaching 20.49%, which is only 3.6% more than the single HC and 77.78% less than the optimum HC-HDZn 10%.

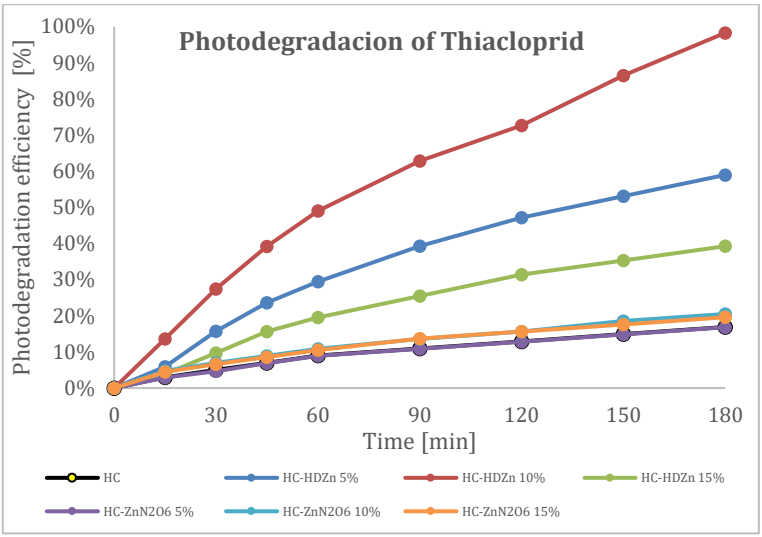

Fig 16. The relationship between the photodegradation efficiency of thiacloprid and the illumination time.

As shown in figure 16, as in the case of metoprolol, the degradation of HC-HDZn 10% is considerably faster than that of other photocatalysts. In contrast to the stabilization observed for metoprolol, thiacloprid shows degradation without signs of stabilization, suggesting that photodegradation may continue if exposure time is prolonged.

The three composites that have shown the highest degradation capacity in the experiment are the HC-HDZn composites, with the 10% by weight being the most efficient, followed by the 5% and thirdly the 15%. As in the previous section, this phenomenon shows that there is no direct relationship between the amount of HDZn combined with HC and the degradation performance. It also requires further studies on the material to justify this fact.

4.6. POLLUTANT DEGRADATION COMPARISON USING THE OPTIMAL PHOTOCATALYST

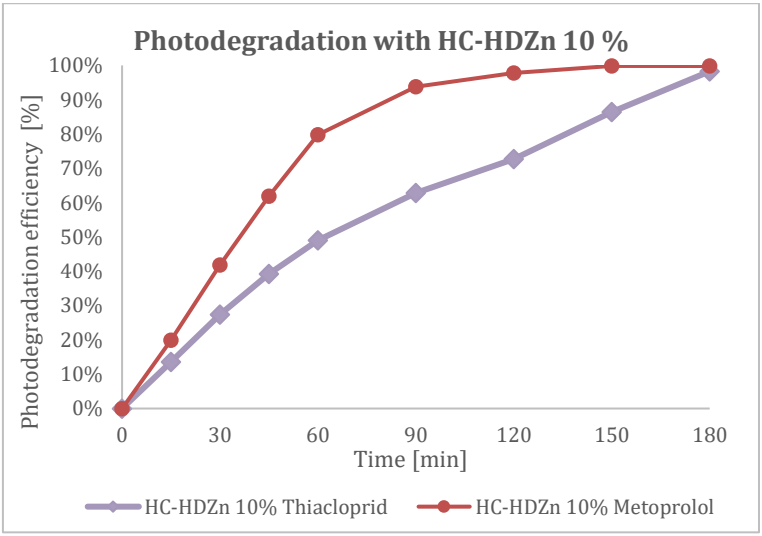

Fig 17. The relationship between the photodegradation efficiency of pollutants using HC-HDZn 10% as photocatalyst.

After the experiments carried out, the optimal photocatalyst (OP) for the degradation of metoprolol and thiacloprid has been determined, in both cases it is the composite HC-HDZn 10%.

As can be seen in the figure 17, HC-HDZn 10% shows a faster and more efficient degradation trend in metoprolol than in thiacloprid. After 3 hours of the photocatalytic process, very similar degradation percentages were achieved, with 99.82% for metoprolol and 98.27% for thiacloprid.

Table 9. Maximum degradation percentage of metoprolol and thiacloprid

	HC	HC-HDZn 5%	HC-HDZn 10%	HC-HDZn 15%	HC-ZnN_2O_6 5%	HC-ZnN_2O_6 10%	HC-ZnN_2O_6 15%
η_M [%]	19.91%	59.90%	99.82%	39.88%	21.96%	23.96%	22.99%
η_T [%]	16.89%	58.96%	98.27%	39.25%	16.82%	20.49%	19.59%

As shown in table 9, it is important to note that, under the same conditions of the photocatalysis process, the degradation of metoprolol using any HC composite presents a higher degree of efficiency compared to the degradation of thiacloprid.

A possible explanation for this phenomenon could be that metoprolol has a higher affinity for HC and a molecular structure more susceptible to photodegradation. Further studies are needed in the future to justify this in more detail.

4.7. ANALYSIS OF PHOTOCATALYST REUSABILITY IN MULTIPLE PHOTOCATALYTIC DEGRADATION CYCLES

In the analysis of the reusability and stability of the optimal photocatalyst, 3 photocatalytic degradation cycles were carried out, each with a duration of 3 hours.

Both OP_M and OP_T (Optimal Photocatalyst) correspond to the same photocatalyst, HC-HDZn 10%.

Table 10. Degradation percentage results after each degradation cycle using HC-HDZn 10%.

	Cycle 1	**Cycle 2**	**Cycle 3**
η_M [%]	99.82%	99.56%	99.30%
η_T [%]	98.27%	96.65%	94.97%

As can be seen in table 10, reuse tests of the optimal photocatalyst (HC-HDZn 10%) showed that it retains at least 90% of its removal capacity after 3 cycles of use.

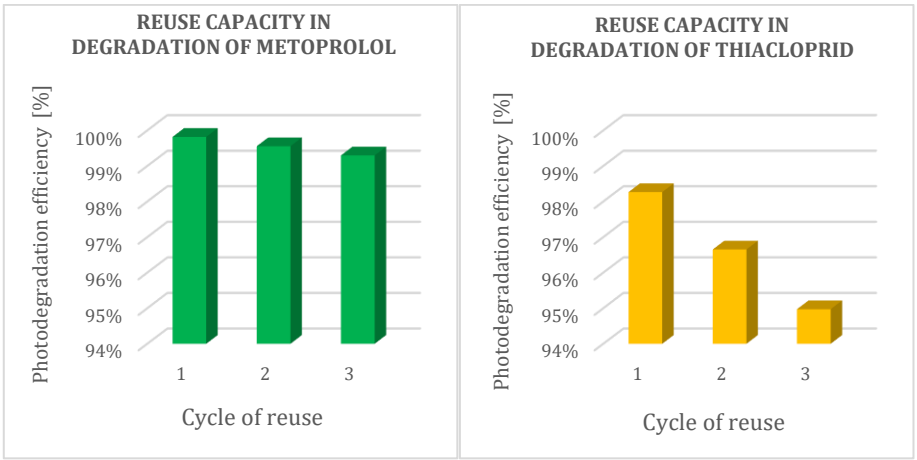

Fig 18-19. Representation of the reuse capacity in the degradation of contaminants.

The degradation efficiency of metoprolol showed a slight decrease over the 3 cycles, decreasing by only 0.52% compared to the initial cycle. In contrast, the degradation of thiacloprid showed a slight decrease of 3.35% in the last cycle compared to the first. This phenomenon indicates that the degradation capacity of the photocatalyst decreases after each reuse cycle.

The results suggest that 10% HC-HDZn exhibits good cyclic stability in reuse tests.

This highlights the future potential of this catalyst, as it proves to be highly efficient even after multiple degradation cycles.

5. CONCLUSIONS

- The degradation of organic pollutants such as metoprolol and thiacloprid is feasible using HC obtained from vine shoots and HC and Zn composites.
- The individual HC has shown efficiency in the heterogeneous photocatalysis process for the mineralization of organic pollutants, achieving the degradation of 19.91% of metoprolol and 16.89% of thiacloprid after a photodegradation period of 3 hours.
- The composite material HC-HDZn 10% achieved the maximum degradation of the pollutants metoprolol and thiacloprid, reaching a maximum percentage of 99.82 % and 98.27 %, respectively, in 3 hours.
- There is no direct relationship between the weight percentage of Zn (either HDZn or ZnN2O6) and the improvement in degradation performance. Among the three composites of 5% to 15% of each, the most successful was the 10% composite.
- The ineffectiveness of vine shoot-derived HC in the adsorption process of metoprolol and thiacloprid pollutants has been demonstrated, as the concentrations of these pollutants remained unchanged after a one-hour adsorption period.
- In the study of the stability and reusability of the optimal photocatalyst HC-HDZn 10%, a degradation percentage of 99.82% was achieved for metoprolol, decreasing slightly to 99.30% after the third cycle. For thiacloprid, degradation was 98.27% in the first cycle, decreasing to 94.97% in the third cycle.
- As possible directions for future research, detailed characterization of the materials is considered essential to justify their performance in heterogeneous photocatalysis. This includes morphological and structural analyses of the HC/Zn composites, as well as studies of the porosity of HC in different composites. The relationship between these characteristics and the observed photocatalytic activity will be investigated. These studies will allow to propose a mechanism for the photocatalytic reaction of HC/Zn composites, providing a deeper understanding of the processes involved and optimizing their application in the degradation of pollutants.

- In addition, it would be relevant to carry out studies on the mineralization of pollutant molecules by Total Organic Carbon (TOC) analysis. This would provide a more direct assessment of the complete mineralization of pollutants into CO_2 and H_2O.

REFERENCES AND NOTES

[1] Promotora dels aliments catalans, El sector del vi a Catalunya, Prodeca, (2021), (https://www.prodeca.cat/sites/default/files/inline-files/Prodeca%20sector%20vi%20a%20Catalunya.pdf).
[2] Institut Català de la Vinya i el Vi, Vi català en xifres, INCAVI, (2024), (https://incavi.gencat.cat/ca/coneix-vi-catala/vi-catala-xifres/).
[3] Institut Català de la Vinya i el Vi, Comercialització denominacions d'origen catalanes, INCAVI, (2022), (https://incavi.gencat.cat/.content/007-coneix-vi-catala/vi-catala-xifres/dades-comercialitzacio/dades-estadistiques/pdf/Comercialitzacio-any-2022.pdf).
[4] Promotora dels aliments catalans, EL SECTOR DEL VI A CATALUNYA, Prodeca, (2024), (https://prodeca.cat/ca/sectors/el-sector-del-vi-catalunya).
[5] Sequera gencat, Què és la sequera, gencat, (2024), (https://sequera.gencat.cat/ca/la-sequera/que-es-la-sequera/).
[6] Agència Catalana de l'Aigua, Estalvi i eficiència de l'aigua, gencat, (2023), (https://aca.gencat.cat/ca/laca/campanyes-i-divulgacio/campanyes/estalvi-i-eficiencia-de-laigua/).
[7] Agència Catalana de l'Aigua, Estat dels embassaments de Catalunya, gencat, (2024), (https://aca.gencat.cat/ca/laigua/consulta-de-dades/dades-obertes/visualitzacio-interactiva-dades/estat-embassaments/).
[8] D.L. Russell, , Tratamiento de aguas residuales : un enfoque práctico, Reverté2012.
[9] R.B. Schäfer, A. Paschke, M. Liess, Aquatic passive sampling of a short-term thiacloprid pulse with the Chemcatcher: Impact of biofouling and use of a diffusion-limiting membrane on the sampling rate, Journal of Chromatography A, 1203 (2008) 1-6.
[10] MCE, Thiacloprid, MedChemExpress, (2024), (https://www.medchemexpress.com/thiacloprid.html?locale=es-ES).
[11] K. Chen, X. Liu, X. Wu, J. Xu, F. Dong, Y. Zheng, The degradation dynamics and rapid detection of thiacloprid and its degradation products in water and soil by UHPLC-QTOF-MS, Chemosphere, 263 (2021) 127960.
[12] A. Stara, M. Pagano, M. Albano, S. Savoca, G. Di Bella, A. Albergamo, Z. Koutkova, M. Sandova, J. Velisek, J. Fabrello, V. Matozzo, C. Faggio, Effects of long-term exposure of Mytilus galloprovincialis to thiacloprid: A multibiomarker approach, Environmental Pollution, 289 (2021) 117892.
[13] J.A. Rodríguez-Liébana, M.D. Mingorance, A. Peña, Thiacloprid adsorption and leaching in soil: Effect of the composition of irrigation solutions, Science of The Total Environment, 610-611 (2018) 367-376.
[14] A.R. Main, N.L. Michel, M.C. Cavallaro, J.V. Headley, K.M. Peru, C.A. Morrissey, Snowmelt transport of neonicotinoid insecticides to Canadian Prairie wetlands, Agriculture, Ecosystems & Environment, 215 (2016) 76-84.

[15] A.W. Schaafsma, V. Limay-Rios, T.S. Baute, J.L. Smith, Neonicotinoid insecticide residues in subsurface drainage and open ditch water around maize fields in southwestern Ontario, PLOS ONE, 14 (2019) e0214787.
[16] L.G. Forero, V. Limay-Rios, Y. Xue, A. Schaafsma, Concentration and movement of neonicotinoids as particulate matter downwind during agricultural practices using air samplers in southwestern Ontario, Canada, Chemosphere, 188 (2017) 130-138.
[17] X.Y. Cai, M. Xu, Y.X. Zhu, Y. Shi, H.W. Wang, Removal of Dinotefuran, Thiacloprid, and Imidaclothiz Neonicotinoids in Water Using a Novel Pseudomonas monteilii FC02-Duckweed (Lemna aequinoctialis) Partnership, Frontiers in microbiology, 13 (2022) 906026.
[18] M.A. Beketov, M. Liess, Acute and delayed effects of the neonicotinoid insecticide thiacloprid on seven freshwater arthropods, Environmental Toxicology and Chemistry, 27 (2008) 461-470.
[19] D. Englert, M. Bundschuh, R. Schulz, Thiacloprid affects trophic interaction between gammarids and mayflies, Environmental Pollution, 167 (2012) 41-46.
[20] J. Velisek, A. Stara, Effect of thiacloprid on early life stages of common carp (Cyprinus carpio), Chemosphere, 194 (2018) 481-487.
[21] R. Freitas, S. Silvestro, M. Pagano, F. Coppola, V. Meucci, F. Battaglia, L. Intorre, A.M.V.M. Soares, C. Pretti, C. Faggio, Impacts of salicylic acid in Mytilus galloprovincialis exposed to warming conditions, Environmental Toxicology and Pharmacology, 80 (2020) 103448.
[22] A. Stara, M. Pagano, G. Capillo, J. Fabrello, M. Sandova, M. Albano, E. Zuskova, J. Velisek, V. Matozzo, C. Faggio, Acute effects of neonicotinoid insecticides on Mytilus galloprovincialis: A case study with the active compound thiacloprid and the commercial formulation calypso 480 SC, Ecotoxicology and Environmental Safety, 203 (2020) 110980.
[23] A. Stara, M. Pagano, G. Capillo, J. Fabrello, M. Sandova, I. Vazzana, E. Zuskova, J. Velisek, V. Matozzo, C. Faggio, Assessing the effects of neonicotinoid insecticide on the bivalve mollusc Mytilus galloprovincialis, Science of The Total Environment, 700 (2020) 134914.
[24] R.S. Vardanyan, V.J. Hruby, 12 - Adrenoblocking Drugs, in: R.S. Vardanyan, V.J. Hruby (Eds.) Synthesis of Essential Drugs, Elsevier, Amsterdam, 2006, pp. 161-177.
[25] WIKIPEDIA, Metoprolol structure, WIKIPEDIA, (2024), (https://en.wikipedia.org/wiki/File:Metoprolol_structure.svg).
[26] X. Yang, R. Zou, K. Tang, H.R. Andersen, I. Angelidaki, Y. Zhang, Degradation of metoprolol from wastewater in a bio-electro-Fenton system, Science of The Total Environment, 771 (2021) 145385.
[27] N. Ouerfelli, N. Vrinceanu, E. Mliki, A.M. Homeida, K.A. Amin, M. Ogrodowczyk, F.S. Alshehri, N. Ouerfelli, Modeling of the irradiation effect on some physicochemical properties of metoprolol tartrate for safe medical uses, Scientific Reports, 10 (2020) 67.
[28] A.C. Alder, C. Schaffner, M. Majewsky, J. Klasmeier, K. Fenner, Fate of β-blocker human pharmaceuticals in surface water: Comparison of measured and simulated concentrations in the Glatt Valley Watershed, Switzerland, Water Research, 44 (2010) 936-948.
[29] Z. Dong, D.B. Senn, R.E. Moran, J.P. Shine, Prioritizing environmental risk of prescription pharmaceuticals, Regulatory Toxicology and Pharmacology, 65 (2013) 60-67.
[30] S.R. Hughes, P. Kay, L.E. Brown, Global Synthesis and Critical Evaluation of Pharmaceutical Data Sets Collected from River Systems, Environmental Science & Technology, 47 (2013) 661-677.
[31] C.N. Brocker, T. Velenosi, H.K. Flaten, G. McWilliams, K. McDaniel, S.K. Shelton, J. Saben, K.W. Krausz, F.J. Gonzalez, A.A. Monte, Metabolomic profiling of metoprolol

hypertension treatment reveals altered gut microbiota-derived urinary metabolites, Human genomics, 14 (2020) 10.
[32] E.-J. van den Brandhof, M. Montforts, Fish embryo toxicity of carbamazepine, diclofenac and metoprolol, Ecotoxicology and Environmental Safety, 73 (2010) 1862-1866.
[33] A. Bin, S. Sobera-Madej, Comparison of the Advanced Oxidation Processes (UV, UV/H2O2 and O3) for the Removal of Antibiotic Substances during Wastewater Treatment, Ozone-science & Engineering - OZONE-SCI ENG, 34 (2012) 136-139.
[34] S. Parsons, Advanced oxidation processes for water and wastewater treatment, IWA publishing2004.
[35] J.C. Castillo Rodríguez, Síntesis y caracterización de compósitos ZrO2-SnO2: efecto de la adición de SnO2 sobre sólidos amorfos de ZrO2 en el proceso de fotodegradación catalítica de fenol en agua, Universidad Autónoma Metropolitana2017.
[36] J.-E. Forero, O.-P. Ortiz, F. Rios, Aplicación de procesos de oxidación avanzada como tratamiento de fenol en aguas residuales industriales de refinería, CT&F Ciencia, Tecnología y Futuro, 3 (2005) 97-109.
[37] R.A.y. Perspectiva, Fotónica del silicio, Gobierno de México, (2019), (https://avanceyperspectiva.cinvestav.mx/fotonica-del-silicio/).
[38] M.E. Borges, M. Sierra, P. Esparza, Solar photocatalysis at semi-pilot scale: wastewater decontamination in a packed-bed photocatalytic reactor system with a visible-solar-light-driven photocatalyst, Clean Technologies and Environmental Policy, 19 (2017) 1239-1245.
[39] M. Lu, Photocatalysis and water purification: from fundamentals to recent applications, John Wiley & Sons2013.
[40] R. Pawar, C. Lee, Heterogeneous Nanocomposite-Photocatalysis for Water Purification, Heterogeneous Nanocomposite-Photocatalysis for Water Purification, (2015) 1-100.
[41] A.O. Ibhadon, P. Fitzpatrick, Heterogeneous Photocatalysis: Recent Advances and Applications, 3 (2013) 189-218.
[42] F. Tzompantzi, C. Tzompantzi-Flores, N.S. Portillo-Vélez, J.C. Castillo-Rodríguez, R. Gómez, R. Pérez Hernández, C.E. Santolalla-Vargas, Preparation and characterization of the polycrystalline material Zn5(OH)6(CO3)2. Determination of the active species in oxide-reduction processes, Fuel, 281 (2020) 118471.
[43] Z. Liu, F. Teng, Understanding the Correlation of Crystal Atoms with Photochemistry Property: Zn5(OH)6(CO3)2 vs. ZnCO3, 3 (2018) 8886-8894.
[44] C. Tzompantzi-Flores, J.C. Castillo-Rodríguez, R. Gómez, F. Tzompantzi, R. Pérez-Hernández, V. De la Luz Tlapaya, C.E. Santolalla-Vargas, Synthesis and characterization of ZnZr composites for the photocatalytic degradation of phenolic molecules: addition effect of ZrO2 over hydrozincite Zn5(OH)6(CO3)2, 94 (2019) 3428-3439.
[45] S. Masoumi, V.B. Borugadda, S. Nanda, A.K. Dalai, Hydrochar: A Review on Its Production Technologies and Applications, 11 (2021) 939.
[46] S. Masoumi, V.B. Borugadda, A.K. Dalai, Biocrude Oil Production via Hydrothermal Liquefaction of Algae and Upgradation Techniques to Liquid Transportation Fuels, in: S. Nanda, D.-V. N. Vo, P.K. Sarangi (Eds.) Biorefinery of Alternative Resources: Targeting Green Fuels and Platform Chemicals, Springer Singapore, Singapore, 2020, pp. 249-270.
[47] S.V. Vassilev, D. Baxter, L.K. Andersen, C.G. Vassileva, An overview of the chemical composition of biomass, Fuel, 89 (2010) 913-933.

[48] F. Zhou, K. Li, F. Hang, Z. Zhang, P. Chen, L. Wei, C. Xie, Efficient removal of methylene blue by activated hydrochar prepared by hydrothermal carbonization and NaOH activation of sugarcane bagasse and phosphoric acid, RSC Advances, 12 (2022) 1885-1896.
[49] J. Fang, L. Zhan, Y.S. Ok, B. Gao, Minireview of potential applications of hydrochar derived from hydrothermal carbonization of biomass, Journal of Industrial and Engineering Chemistry, 57 (2018) 15-21.
[50] J.O. Ighalo, S. Rangabhashiyam, K. Dulta, C.T. Umeh, K.O. Iwuozor, C.O. Aniagor, S.O. Eshiemogie, F.U. Iwuchukwu, C.A. Igwegbe, Recent advances in hydrochar application for the adsorptive removal of wastewater pollutants, Chemical Engineering Research and Design, 184 (2022) 419-456.
[51] J.A. Libra, K.S. Ro, C. Kammann, A. Funke, N.D. Berge, Y. Neubauer, M.-M. Titirici, C. Fühner, O. Bens, J. Kern, K.-H. Emmerich, Hydrothermal carbonization of biomass residuals: a comparative review of the chemistry, processes and applications of wet and dry pyrolysis, Biofuels, 2 (2011) 71-106.
[52] Z. Hu, Z. Shen, J.C. Yu, Converting Carbohydrates to Carbon-Based Photocatalysts for Environmental Treatment, Environmental Science & Technology, 51 (2017) 7076-7083.
[53] M.T. Islam, A.I. Sultana, C. Chambers, S. Saha, N. Saha, K. Kirtania, M.T. Reza, Recent Progress on Emerging Applications of Hydrochar, 15 (2022) 9340.
[54] M. Manga, C. Aragón-Briceño, P. Boutikos, S. Semiyaga, O. Olabinjo, C.C. Muoghalu, Biochar and Its Potential Application for the Improvement of the Anaerobic Digestion Process: A Critical Review, 16 (2023) 4051.
[55] A.A. Azzaz, B. Khiari, S. Jellali, C.M. Ghimbeu, M. Jeguirim, Hydrochars production, characterization and application for wastewater treatment: A review, Renewable and Sustainable Energy Reviews, 127 (2020) 109882.
[56] M. Jalilian, R. Bissessur, M. Ahmed, A. Hsiao, Q.S. He, Y. Hu, A review: Hydrochar as potential adsorbents for wastewater treatment and CO2 adsorption, Science of The Total Environment, 914 (2024) 169823.
[57] M.K. Gautam, T. Mondal, R. Nath, B. Mahajon, M. Chincholikar, A. Bose, D. Das, R. Das, S. Mondal, Harnessing Activated Hydrochars: A Novel Approach for Pharmaceutical Contaminant Removal, 10 (2024) 8.
[58] S. Li, Q. Ma, L. Chen, Z. Yang, M. Aqeel Kamran, B. Chen, Hydrochar-mediated photocatalyst Fe3O4/BiOBr@HC for highly efficient carbamazepine degradation under visible LED light irradiation, Chemical Engineering Journal, 433 (2022) 134492.
[59] R.P. Cavalcante, R.F. Dantas, B. Bayarri, O. González, J. Giménez, S. Esplugas, A. Machulek, Synthesis and characterization of B-doped TiO2 and their performance for the degradation of metoprolol, Catalysis Today, 252 (2015) 27-34.

ACRONYMS

HC	Hydrochar
HDZn/$Zn_5(CO_3)_2(OH)_6$	Hydrozincite
ZnN2O6	Zinc Nitrate
HTC	Hydrothermal Carbonization
AOPs	Advances Oxidation Processes
PPCP	Pharmaceuticals and Personal Care Products
POPs	Persistent Organic Pollutants
UV	Ultraviolet
e-	Electron
h+	Hole
hv	Photon energy
M	Metoprolol
T	Thiacloprid
C	Concentration
η	Photodegradation efficiency
·OH	Hydroxyl radical
O_2^-	Superoxide radical
·OOH	Hydroperoxyl radical
H_2O_2	Hydrogen peroxide
TiO_2	Titanium dioxide

APPENDICES

APPENDIX 1: TABLE OF CONTAMINANT CONCENTRATIONS

Table 11. Variation of metoprolol concentration in the degradation using different photocatalysts.

	HC	**HC-HDZn 5%**	**HC-HDZn 10%**	**HC-HDZn 15%**	**HC-ZnN2O6 5%**	**HC-ZnN2O6 10%**	**HC-ZnN2O6 15%**
Time [min]	C_M [ppm]	C_M [ppm]	C_M [ppm]	C_M [ppm]	C_M [ppm]	C_M [ppm]	C_M [ppm]
0	5.0058	5.0096	5.0080	5.0080	5.0088	5.0088	5.0099
15	4.8111	4.5083	4.0088	4.8111	4.7084	4.6083	4.6584
30	4.5083	3.5093	2.9109	4.3112	4.4093	4.3092	4.3592
45	4.3116	2.8096	1.9101	4.0113	4.2093	4.1093	4.1593
60	4.2091	2.5097	1.0100	3.7110	4.1093	4.0088	4.0589
90	4.1090	2.2091	0.3103	3.3114	4.0092	3.9086	3.9080
120	4.0589	2.0592	0.1102	3.1099	3.9592	3.8587	3.8543
150	4.0087	2.0082	0.0102	3.0111	3.9109	3.8090	3.8576
180	4.0091	2.0089	0.0091	3.0111	3.9087	3.8086	3.8580

Table 12. Variation of thiacloprid concentration in the degradation using different photocatalysts.

	HC	HC-HDZn 5%	HC-HDZn 10%	HC-HDZn 15%	HC-ZnN2O6 5%	HC-ZnN2O6 10%	HC-ZnN2O6 15%
Time [min]	C_T [ppm]	C_T [ppm]	C_T [ppm]	C_T [ppm]	C_T [ppm]	C_T [ppm]	C_T [ppm]
0	5.0337	5.0826	5.0731	5.0774	5.0288	5.0736	5.0779
15	4.8828	4.7829	4.3833	4.8828	4.8825	4.8326	4.8525
30	4.7829	4.2834	3.6841	4.5831	4.7960	4.7227	4.7414
45	4.6830	3.8839	3.0847	4.2834	4.6829	4.6229	4.6426
60	4.5831	3.5842	2.5853	4.0837	4.5830	4.5230	4.5427
90	4.4832	3.0847	1.8860	3.7840	4.4832	4.3833	4.3830
120	4.3833	2.6851	1.3865	3.4843	4.3834	4.2797	4.2832
150	4.2834	2.3855	0.6873	3.2845	4.2835	4.1337	4.1832
180	4.1835	2.0858	0.0879	3.0847	4.1828	4.0338	4.0834

Table 13. Variation of pollutant concentration in the 3 cycles.

	Concentration Metoprolol [ppm]			Concentration Thiacloprid [ppm]		
Time [min]	C1	C2	C3	C1	C2	C3
0	5.0090	5.0090	5.0090	5.0715	5.0715	5.0715
180	0.0091	0.0223	0.0352	0.0879	0.1698	0.2550

APPENDIX 2: ANALYSIS OF THE BAND GAP ENERGY OF HC-HDZN

In a study carried out by the research group, the values of the band gap energies of the reference materials (HC) and the HC-HDZn composite materials were determined using the UV-Vis Diffuse Reflectance Spectroscopy technique, the results of which are shown in figure 20. According to the results obtained, the band gap energies of the materials are in the range of 4.6 to 2.7 eV. Since the bandgap energy of HC is the highest, it is considered that this material acts as an insulator.

The material with the highest photocatalytic activity, HC-HDZn 10%, has a bandgap energy of 3.2 eV, which is within the typical range of semiconductors.

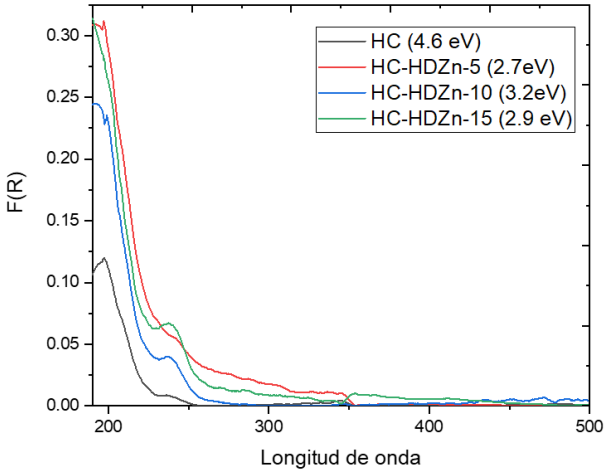

Fig 20. UV-Vis diffuse reflectance spectroscopy analysis of materials synthesized with HC-HDZn.